XLI CILAMCE
XLI Ibero-Latin American Congress on Computational Methods in Engineering
16-19 November, 2020 FOZ DO IGUAÇU PARANÁ - BRAZIL

# Numerical investigation of bifurcation instability in constrained minimization problem of elasticity

Adair R. Aguiar[1], Lucas A. Rocha[1]

[1]*Department of Structural Engineering, São Carlos School of Engineering, University of São Paulo*
*Av. Trabalhador Sãocarlense, 400, Cx. P. 359, 13560-590, São Carlos - SP - Brazil*
*aguiarar@sc.usp.br , lucas.almeida.rocha@usp.br*

**Abstract.** There are problems in classical linear elasticity whose closed form solutions, while satisfying the governing equations of equilibrium and well-posed boundary conditions, predict material overlapping, which is not physically realistic. One possible way to prevent this anomalous behavior is to consider the minimization of the total potential energy of classical linear elasticity subjected to the local injectivity constraint. In two dimensions, the corresponding constrained minimization problem has a solution, which may not be unique. To investigate this class of problems, we consider the equilibrium problem of a cylindrically anisotropic disk subjected to a prescribed displacement along its boundary. We search numerically for either radially or rotationally symmetric solutions defined in a one-dimensional domain. Our discretization strategy uses linear finite elements and yields convergent sequences of solutions at a very low computational cost when compared to results reported in the literature. It is clear from our investigation that a small perturbation must be introduced to obtain the rotationally symmetric solution, for otherwise the solution obtained is radially symmetric. The total potential energy from the rotationally symmetric solution is lower than the corresponding energy evaluated from the radially symmetric solution.

**Keywords:** Anisotropy, Elasticity, Constraint minimization, Penalty method, Finite element method

## 1 Introduction

There are problems in classical linear elasticity whose closed form solutions, while satisfying the governing equations of equilibrium and well-posed boundary conditions, predict material overlapping, which, of course, is not physically realistic. Mathematically, material overlapping is characterized by the loss of injectivity of the deformation field. Locally, it means that the determinant of the deformation gradient is not positive. This anomalous behavior is usually associated with singular stresses and strains, which contradict the basic assumption of linear elasticity that the displacement gradient is infinitesimal.

The anomalous behavior may appear at interior points of linearly elastic anisotropic disks in equilibrium in the absence of body force and under external pressure. The associated problems are simple enough to yield closed form solutions against which numerical solutions can be compared and validated and, at the same time, be used to better understand the role of injectivity in elasticity. Closed form solutions were obtained by Lekhnitskii [1] and later discussed by Fosdick and Royer-Carfagni [2] in the context of classical linear elasticity. These solutions predict not only material overlapping, but also stress singularities for materials with elastic modulus in the radial direction being greater than the elastic modulus in the tangential direction. Christensen [3] has argued that material properties of this type are found in carbon fibers with radial microstructure.

To prevent the anomalous behavior in plane problems of elasticity, Fosdick and Royer-Carfagni [2] propose to minimize the classical energy functional of linear elasticity subject to a local injectivity constraint, which consists of imposing that the determinant of the deformation gradient be no less than a small positive parameter. They show that under suitable, but otherwise sufficiently general boundary conditions, a solution exists. Our aim is to investigate the existence of non unique solutions for this class of minimization problems. In view of its simple theoretical structure, we consider the class of disk problems mentioned above in the context of the constrained minimization theory of Fosdick and Royer-Carfagni [2]. In this context, these authors have found a closed form solution that is radially symmetric with respect to the center of the disk, is different from the radially symmetric solution of classical linear elasticity, and satisfies the injectivity constraint.

In general, however, the associated constrained minimization problems are highly nonlinear and require a numerical solution. Aguiar [4] proposes a numerical approach based on an interior penalty formulation, which is simple and precludes the necessity of knowing the active region in advance. The approach consists of searching for minimizers of a penalized energy functional $\mathcal{E}_\delta = \mathcal{E} + \mathcal{P}/\delta$, where $\mathcal{E}$ is the total potential energy of linear elasticity, $\delta$ is an arbitrary positive number, and $\mathcal{P}$ is a non-negative functional defined on a constraint set $\mathcal{A}_\varepsilon$, which is the set of all admissible deformations that satisfy the local injectivity constraint. A minimizing sequence of solutions parameterized by $\delta$ is then constructed, which tends to the solution of the constrained minimization problem as $\delta$ tends to $\infty$. Even though the associated minimization problem is still a constrained problem, because minimizers are searched in the constraint set $\mathcal{A}_\epsilon$, from a computational point of view, this problem can be treated as an unconstrained minimization problem and solved by standard nonlinear programming techniques.

Using both the penalty formulation proposed by Aguiar [4] and a very fine mesh of isoparametric biquadratic finite elements, Fosdick et al. [5] have found that a secondary solution is possible for low enough shear modulus. This solution seems to be rotationally symmetric with respect to the center of the disk and bifurcates from the radially symmetric solution found previously by Fosdick and Royer-Carfagni [2]. The geometry-related error induced by the boundary approximation acts as a perturbation in the search of a stable equilibrium solution.

In this work we also use the penalty formulation of Aguiar [4] and assume that solutions of the constrained minimization problem are either radially or rotationally symmetric, which allow us to consider linear finite elements defined in a one-dimensional domain, rather than in the two-dimensional domain considered by Fosdick et al. [5]. Thus, there is no boundary approximation and, therefore, we only obtain the radially symmetric solution in the absence of perturbations. To obtain the secondary solution, we add a perturbation to the initial candidate for a minimizer in the minimization procedure. Our approach yields convergent sequences of numerical solutions at a very low computational cost. The numerical solutions converge to a limit function that is different from the numerical solution reported in Fosdick et al. [5]. In addition, it sheds light on the behavior of the secondary solution that is not reported in this previous work. Our numerical results show that the tangential displacement field is linear near the center of the disk and that the total potential energy from this secondary solution is lower than the corresponding energy evaluated from the radially symmetric solution.

In Section 2 we apply the numerical procedure proposed by Aguiar [4], which is based on an interior penalty formulation together with a finite element scheme, to the class of constrained minimization problems considered by Fosdick and Royer-Carfagni [2] with the goal of determining an approximate minimizer for this class of problems. In Section 3 we consider the equilibrium problem of a cylindrically anisotropic disk subjected to a prescribed displacement along its boundary and obtain the energy functional $\mathcal{E}$ and the penalty functional $\mathcal{P}$. In Section 4 we show graphs of convergent sequences of numerical results concerning a secondary solution of the associated constrained minimization problem. In Section 5 we present some concluding remarks.

## 2 Numerical procedure

Let $\mathcal{B} \subset \mathbb{R}^2$ be the undistorted natural reference configuration of the body. Points $\mathbf{X} \in \mathcal{B}$ are mapped to points $\mathbf{x} \equiv \mathbf{f}(\mathbf{X}) = \mathbf{X} + \mathbf{u}(\mathbf{X})$, $\mathbf{x} \in \mathbb{R}^2$, where $\mathbf{u}(\mathbf{X})$ is the displacement of $\mathbf{X}$. The boundary $\partial\mathcal{B}$ of $\mathcal{B}$ is composed of two non-intersecting parts, $\partial_1\mathcal{B}$ and $\partial_2\mathcal{B}$, $\partial\mathcal{B} = \partial_1\mathcal{B}\cup\partial_2\mathcal{B}$, $\partial_1\mathcal{B}\cap\partial_2\mathcal{B} = \emptyset$, such that $\mathbf{u}(\mathbf{X}) = \bar{\mathbf{u}}(\mathbf{X})$ for $\mathbf{X} \in \partial_1\mathcal{B}$, where $\bar{\mathbf{u}}$ is a given function, and a dead load traction field $\bar{\mathbf{t}}(\mathbf{X})$ is prescribed for $\mathbf{X} \in \partial_2\mathcal{B}$. In addition, a body force $\mathbf{b}(\mathbf{X})$ per unit of volume acts on $\mathbf{X} \in \mathcal{B}$.

We consider the problem of minimization of the total potential energy of classical linear elasticity, given by

$$\min_{\mathbf{v}\in\mathcal{A}_\varepsilon} \mathcal{E}[\mathbf{v}], \qquad \mathcal{E}[\mathbf{v}] = \frac{1}{2}\int_{\mathcal{B}} \mathbb{C}[\mathbf{E}]\cdot\mathbf{E}\,d\mathbf{X} - \int_{\mathcal{B}} \mathbf{b}\cdot\mathbf{v}\,d\mathbf{X} - \int_{\partial_2\mathcal{B}} \bar{\mathbf{t}}\cdot\mathbf{v}\,d\mathbf{X}\,, \tag{1}$$

where $\mathbf{E} = (\nabla\mathbf{v} + \nabla\mathbf{v}^T)/2$ is the infinitesimal strain tensor field and

$$\mathcal{A}_\varepsilon \equiv \left\{\mathbf{v} : \mathcal{W}^{1,2}(\mathcal{B}) \to \mathbb{R}^2 \,|\, \det(\mathbf{1} + \nabla\mathbf{v}) \geq \varepsilon > 0,\, \mathbf{v}(\mathbf{X}) = \bar{\mathbf{u}}(\mathbf{X}) \text{ for } \mathbf{X} \in \partial_1\mathcal{B}\right\} \tag{2}$$

is the set of admissible displacement fields, with $\varepsilon$ being a sufficiently small positive scalar. Furthermore, $\mathbb{C}$ is the elasticity tensor, which is symmetric and positive definite. If the injectivity constraint $\det(\mathbf{1} + \nabla\mathbf{v}) \geq \varepsilon > 0$ were not present, the constrained minimization problem stated above would become the classical minimization problem of linear elasticity theory.

Let $\mathbf{u} \in \mathcal{A}_\varepsilon$ be the minimizer of $\mathcal{E}[\cdot]$ and $\mathcal{B}$ be divided in two open subregions $\mathcal{B}_>$ and $\mathcal{B}_=$, such that $\mathcal{B} = \mathcal{B}_> \cup \mathcal{B}_= \cup \Sigma$ and $\mathcal{B}_> \cap \mathcal{B}_= = \emptyset$, where $\Sigma$ is the interface between $\mathcal{B}_>$ and $\mathcal{B}_=$. The subregions $\mathcal{B}_>$ and $\mathcal{B}_=$ are defined as

$$\mathcal{B}_> \equiv \text{int}[\{\mathbf{X} \in \mathcal{B} \mid \det\nabla\mathbf{f}(\mathbf{X}) > \varepsilon\}], \qquad \mathcal{B}_= \equiv \text{int}[\{\mathbf{X} \in \mathcal{B} \mid \det\nabla\mathbf{f}(\mathbf{X}) = \varepsilon\}], \tag{3}$$

where $\mathrm{int}[\cdot]$ denotes the interior of a set. Fosdick and Royer-Carfagni [2] show that the Euler-Lagrange equations for the constrained minimization problem defined by Eq. (1) together with Eq. (2) are given by

$$\mathrm{Div}\,\mathbf{T} + \mathbf{b} = \mathbf{0} \quad \text{in } \mathcal{B}_{>}\,, \qquad \mathrm{Div}\,(\mathbf{T} - \varepsilon\lambda(\nabla\mathbf{f})^{-T}) + \mathbf{b} = \mathbf{0} \quad \text{in } \mathcal{B}_{=}\,, \tag{4}$$

where $\lambda(\mathbf{X}) \geq 0$ is the Lagrange multiplier field associated with the injectivity constraint $\det(\mathbf{1} + \nabla\mathbf{u}) \geq \varepsilon > 0$ and $\mathbf{T} = \mathbb{C}[\mathbf{E}]$ is the stress tensor. The boundary conditions are given by

$$\mathbf{T}\,\mathbf{n} = \bar{\mathbf{t}} \quad \text{in } \partial_2\mathcal{B}_{>}\,, \qquad (\mathbf{T} - \varepsilon\lambda(\nabla\mathbf{f})^{-T})\,\mathbf{n} = \bar{\mathbf{t}} \quad \text{in } \partial_2\mathcal{B}_{=}\,, \tag{5}$$

where $\mathbf{n}$ is a unit normal to $\partial_2\mathcal{B}$. In addition, the jump condition

$$(\mathbf{T} - \varepsilon\lambda(\nabla\mathbf{f})^{-T})|_{\Sigma\cap\bar{\mathcal{B}}_{=}}\,\mathbf{n} = \mathbf{T}|_{\Sigma\cap\bar{\mathcal{B}}_{>}}\,\mathbf{n} \tag{6}$$

must hold across $\Sigma \equiv \bar{\mathcal{B}}_{>} \cap \bar{\mathcal{B}}_{=}$, where $\mathbf{n}$ is a unit normal to $\Sigma$ and where $\Sigma \cap \bar{\mathcal{B}}_{=}$ and $\Sigma \cap \bar{\mathcal{B}}_{>}$ mean that the evaluations are understood as limits to the dividing interface $\Sigma$ from within $\mathcal{B}_{=}$ and $\mathcal{B}_{>}$, respectively.

In the interior penalty method, we replace the the energy functional of Eq. (1b) by a penalized potential energy functional $\mathcal{E}_\delta : \mathcal{A}_\varepsilon \to \mathbb{R}$ defined by

$$\mathcal{E}_\delta[\mathbf{u}] \equiv \mathcal{E}[\mathbf{u}] + \frac{1}{\delta}\mathcal{P}[\mathbf{u}], \tag{7}$$

where $\delta > 0$ is a penalty parameter and $\mathcal{P}[\mathbf{u}] : \mathcal{A}_\varepsilon \to \mathbb{R}$ is a barrier functional, which must satisfy $\mathcal{P}[\mathbf{u}] > 0, \forall\,\mathbf{u} \in \mathcal{A}_\varepsilon$, and $\mathcal{P}[\mathbf{u}] \to \infty$ as $\mathbf{u}$ approaches the boundary of $\mathcal{A}_\varepsilon$. The addition of the term $\mathcal{P}/\delta$ establishes a barrier on the boundary of the constraint set $\mathcal{A}_\varepsilon$ that prevents the minimizing procedure from leaving the set $\mathcal{A}_\varepsilon$. We then solve a sequence of minimization problems of the form

$$\min_{\mathbf{v}\in\mathcal{A}_\varepsilon} \mathcal{E}_\delta[\mathbf{v}] \tag{8}$$

for increasingly higher values of $\delta$.

Let $\mathbf{u}_\delta$ denote a minimizer of Eq. (8). We expect that, in the limit as $\delta \to \infty$, the sequence $\{\mathbf{u}_\delta\}$ yields a limit function that is a solution of the original constrained minimization problem defined by Eq. (1) together with Eq. (2). In this work, we consider the same barrier functional proposed by Aguiar [4] and used by Fosdick et al. [5], which is given by

$$\mathcal{P}[\mathbf{u}] \equiv \int_{\mathcal{B}} \frac{1}{\det(\mathbf{1} + \nabla\mathbf{u}) - \varepsilon}\,d\mathbf{X}, \qquad \forall\mathbf{u} \in \mathcal{A}_\varepsilon. \tag{9}$$

We expect that the Lagrange multiplier $\lambda$ that appears in the Eqs. (4)-(6) is the limit function of the sequence $\{\lambda_\delta\}$, where, according to Aguiar [4],

$$\lambda_\delta = \left[\delta\,(\det(\mathbf{1} + \nabla\mathbf{u}) - \varepsilon)^2\right]^{-1}. \tag{10}$$

To solve numerically the minimization problem defined by Eq. (8) together with Eq. (7), Eq. (1b), and Eq. (9), we consider a finite element formulation of this problem. It consists of determining an approximate minimizer for Eq. (8) that belongs to a finite dimensional subspace $\mathcal{A}_h \subset \mathcal{A}_\varepsilon$ spanned by a set of vector-valued basis functions $\{\mathbf{\Phi}_i\}$, where $h$ stands for the characteristic length of the finite element. We expect that, as $h \to 0$, this approximate minimizer tends to $\mathbf{u}_\delta$. Therefore, in Eq. (8), we consider only displacement fields $\mathbf{v}_h \in \mathcal{A}_\varepsilon$ of the form

$$\mathbf{v}_h = \sum_{i=1}^{m} s_i\mathbf{\Phi}_i, \tag{11}$$

where $s_i \in \mathbb{R}, i = 1, 2, ..., m$ is a degree of freedom and $m$ is the total number of degrees of freedom associated with the discretization. Let us introduce the vector $\mathbf{s} \equiv (s_1, s_2, ..., s_m)$ and the functions $\mathcal{E}_h(\mathbf{s}) \equiv \mathcal{E}[\mathbf{v}_h]$ and $\mathcal{P}_h(\mathbf{s}) \equiv \mathcal{P}[\mathbf{v}_h]$. Then, the discrete version of the penalized potential in Eq. (7) is defined by

$$\mathcal{F}_\delta(\mathbf{s}) \equiv \mathcal{E}_h(\mathbf{s}) + \frac{1}{\delta}\mathcal{P}_h(\mathbf{s}) \tag{12}$$

and the associated discrete minimization problem is given by

$$\min_{\mathbf{s}\in\mathbb{R}^m} \mathcal{F}_\delta(\mathbf{s}) \tag{13}$$

subject to $\det(\mathbf{1} + \nabla \mathbf{v}_h) \geq \varepsilon > 0$ in parts of the domain where $\mathbf{v}_h$ is smooth. This minimization problem is solved iteratively by the numerical procedure proposed by Aguiar [4], which is based on a standard unconstrained minimization method with a line search technique.

In summary, starting from an initial guess $\mathbf{s}_0$ and a penalty parameter $\delta$, we use the numerical procedure of Aguiar [4] to generate a sequence of approximations $\{\mathbf{s}_k\}$, $k = 1, 2, 3, ...$, which converges to the solution of the discrete minimization problem in Eq. (13). Next, we increase $\delta$ and minimize again the corresponding functional $\mathcal{F}_\delta$. However, this time we take $\mathbf{s}_0$ to be the solution obtained from the previous $\delta$. As $\delta \to \infty$, the solution obtained for the discrete minimization problem, given by Eq. (13), tends to an approximate solution $\mathbf{u}_h \in \mathcal{V}_h$ of the original minimization problem, given by Eq. (1). By letting $h \to 0$, we generate a sequence of approximations $\{\mathbf{u}_h\}$ that converges to the minimizer of the original problem in Eq. (1).

## 3 Problem formulation

We consider the problem of an anisotropic disk of radius $R_e$ in equilibrium in the absence of body force. The external boundary $\partial\mathcal{B}$ is subjected to a prescribed displacement $\bar{\mathbf{u}} = \bar{u}_r\, \mathbf{e}_r + \bar{u}_\theta\, \mathbf{e}_\theta$, where $\{\mathbf{e}_r, \mathbf{e}_\theta\}$ is an orthonormal basis associated to the polar coordinate system $(R, \Theta)$. In addition, the displacement field is null at the center of the disk.

Relative to the basis $\{\mathbf{e}_r, \mathbf{e}_\theta\}$ at a material point $\mathbf{X} = R\, \mathbf{e}_r \in \mathcal{B}$, the stress and the strain tensors of classical linear elasticity are given by, respectively,

$$\mathbf{T} = \sigma_{rr}\, \mathbf{e}_r \otimes \mathbf{e}_r + \sigma_{\theta\theta}\, \mathbf{e}_\theta \otimes \mathbf{e}_\theta + \sigma_{r\theta}\, (\mathbf{e}_r \otimes \mathbf{e}_\theta + \mathbf{e}_\theta \otimes \mathbf{e}_r)\,, \tag{14}$$

$$\mathbf{E} = \epsilon_{rr}\, \mathbf{e}_r \otimes \mathbf{e}_r + \epsilon_{\theta\theta}\, \mathbf{e}_\theta \otimes \mathbf{e}_\theta + \epsilon_{r\theta}\, (\mathbf{e}_r \otimes \mathbf{e}_\theta + \mathbf{e}_\theta \otimes \mathbf{e}_r) \tag{15}$$

and are related to each other through the Generalized Hooke's Law, $\mathbf{T} = \mathbb{C}[\mathbf{E}]$, which, here, yields the nonzero components

$$\sigma_{rr} = c_{11}\epsilon_{rr} + c_{12}\epsilon_{\theta\theta}, \qquad \sigma_{\theta\theta} = c_{12}\epsilon_{rr} + c_{22}\epsilon_{\theta\theta}, \qquad \sigma_{r\theta} = 2c_{66}\epsilon_{r\theta}, \tag{16}$$

with $c_{11}, c_{22}, c_{12}$ and $c_{66}$ being the elastic moduli.

We assume that the displacement field is rotationally symmetric with respect to the center of the disk, yielding

$$\mathbf{u}(R, \Theta) = u_r(R)\, \mathbf{e}_r + u_\theta(R)\, \mathbf{e}_\theta. \tag{17}$$

Therefore, the strain components are given by

$$\epsilon_{rr} = u_r', \qquad \epsilon_{\theta\theta} = \frac{u_r}{R}, \qquad \epsilon_{r\theta} = \frac{1}{2}\left(u_\theta' - \frac{u_\theta}{R}\right), \tag{18}$$

and the determinant of the deformation gradient by

$$\det(\mathbf{1} + \nabla \mathbf{u}) = (1 + u_r')(1 + u_r/R) + u_\theta'\, u_\theta/R, \tag{19}$$

where $(\cdot)' \equiv d(\cdot)/dR$.

It follows from Eqs. (14)-(18) that the total potential energy functional $\mathcal{E}$, given by Eq. (1b), and the barrier functional $\mathcal{P}$, given by Eq. (9), can be written as, respectively,

$$\mathcal{E}[\mathbf{u}] = \pi \int_0^{R_e} \left[ c_{11}\, R\, (u_r')^2 + 2c_{12}\, u_r\, u_r' + c_{22}\frac{u_r^2}{R} + c_{66}\, R\, (u_\theta')^2 - 2c_{66}\, u_\theta\, u_\theta' + c_{66}\frac{u_\theta^2}{R} \right] dR\,, \tag{20}$$

$$\mathcal{P}[\mathbf{u}] = 2\pi \int_0^{R_e} \frac{R}{(1 + u_r')\,(1 + u_r/R) + u_\theta'\, u_\theta/R - \varepsilon}\, dR. \tag{21}$$

## 4 Numerical results

We apply the numerical procedure described in Section 2 to solve numerically the disk problem formulated in Section 3. We have chosen the same material and geometric parameters that Fosdick et al. [5] used in their investigation on the existence of a secondary solution of the disk problem. In dimensionless units, $\bar{u}_r \equiv \bar{\mathbf{u}} \cdot \mathbf{e}_r = -0.05$, $\bar{u}_\theta \equiv \bar{\mathbf{u}} \cdot \mathbf{e}_\theta = 0$, $c_{11} = 10^5$, $c_{22} = 10^4$, $c_{12} = 10^3$, $c_{66} = 10^3$, $\varepsilon = 0.1$ and $R_e = 1$.

We have considered a sequence of uniform meshes with $N$ linear finite elements, where $N \in \{256, 1024, 4096, 16384, 65536\}$, and the sequence of penalty parameters $\delta \in \{10^{-3}, 10^{-2}, 10^{-1}, 10^0, ..., 10^8\}$. Our numerical experiments have confirmed that the numerical results do not change significantly for $\delta > 10^8$.

The choice of the initial candidate for a minimizer is crucial for obtaining a secondary solution, which, in this work, is rotationally symmetric with respect to the center of the disk. First, we consider that this candidate is the solution of the unconstrained problem of an isotropic disk, i.e., $\mathbf{u} = (R/R_e)\,\bar{u}_r\,\mathbf{e}_r$. This solution yields the initial guess $\mathbf{s}_0$ through Eq. (11), where, here, $m = 2\,M$, with $M$ being the number of mesh nodes. In this respect, the components of $\mathbf{s}_0$ are $s_0^{2\,i-1} \equiv \mathbf{u}(R_i)\cdot\mathbf{e}_r = -0.05\,R_i$ and $s_0^{2\,i} \equiv \mathbf{u}(R_i)\cdot\mathbf{e}_\theta = 0$, where $i = 1, 2, 3, ..., M$, and $R_i$ denotes the position of the $i$-th node. Using this initial guess, which was also used by Fosdick et al. [5], we obtain a convergent sequence of numerical solutions that tends to the radially symmetric solution determined analytically by Fosdick and Royer-Carfagni [2].

To obtain a secondary solution, we introduce a perturbation $u_\theta^0$ in the tangential displacement. Specifically, except for the prescribed value on the boundary, given by $\bar{u}_\theta$, all the components of the initial guess $\mathbf{s}_0$ associated to the tangential displacement are set equal to $u_\theta^0$. We then have that $s_0^{2\,i} = u_\theta^0$, $i = 2, \ldots, M-1$ with $R_1 = 0$ and $R_M = R_e$. Here, we use $u_\theta^0 = 10^{-5}$, because it is the minimum perturbation necessary to obtain a secondary solution for the mesh with 256 elements. Smaller values of $u_\theta^0$ could be used for the more refined meshes.

By approximating the circular boundary of the domain with quadratic polynomials from a $\mathcal{Q}_2$ isoparametric finite element discretization, Fosdick et al. [5] have also introduced a perturbation, which is small. As a result, their secondary solution could only be obtained with a very fine mesh. In our case, we control explicitly the size of the perturbation $u_\theta^0$, allowing to obtain the secondary solution with a coarse mesh.

The interior penalty method requires that the initial guess must satisfy the local injectivity constraint. It is not clear *a priori* that the perturbed initial guess we use is locally injective. In fact, large values of $u_\theta^0$ can make the initial guess to violate the constraint; especially in the case of fine meshes. Therefore, we check for this violation at all quadrature points before we start the search procedure.

In Fig. 1 we show solid lines representing the radial displacement $u_r$ of the rotationally symmetric solution obtained from each one of the five meshes for a fixed large penalty parameter $\delta$. We also show a dashed line representing $u_r$ of the radially symmetric solution from the constrained theory of Fosdick and Royer-Carfagni [2]. Figure 1a refers to the whole domain $(0, R_e)$ and Fig. 1b refers to a vicinity of the origin. We see from these figures that the rotationally symmetric solutions yield a sequence of radial displacements that converge to a limit function, which is, in modulus, greater than the modulus of its radially symmetric counterpart. Even though it is not shown in Fig. 1, this limit function is very close to $u_r$ of the radially symmetric solution from the unconstrained classical linear theory. These observations represent a major difference between our results and the ones reported in Fosdick et al. [5]. Without presenting convergence analysis, these authors show results indicating that their $u_r$ from the numerical solution is close to $u_r$ of the radially symmetric solution from the constrained theory.

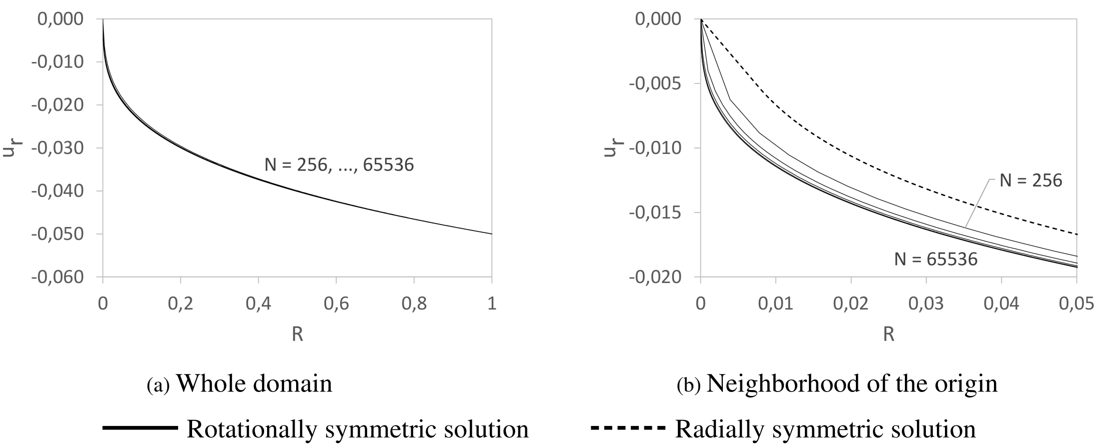


Figure 1. Radial displacement $u_r$ obtained analytically (dashed line) and numerically (solid lines) using $256, 1024, 4096, 16384, 65536$ elements and $\delta = 10^8$.

In Fig. 2 we show curves for the tangential displacement $u_\theta$ obtained from the five uniform meshes and a fixed large penalty parameter $\delta$. Recall from the exposition above that $u_\theta = 0$ in the case of the radially symmetric solution of Fosdick and Royer-Carfagni [2]. The results are presented in two scales, so that Fig. 2a refers to the entire interval $(0, R_e)$ and Fig. 2b refers to a vicinity of the origin. We see from Fig. 2b that the numerical approximations of $u_\theta$ converge to a limit function as the number of elements $N$ increases. This limit function is linear near the center of the disk, increases nonlinearly as $R$ increases, reaches a maximum value at approximately $R = 0.0152$, and then decreases monotonically for larger values of $R$. In the region where the limit function is linear we have used 144 elements for the most refined mesh of 65536 elements.

The above results are qualitatively similar to the corresponding results presented by Fosdick et al. [5] in their

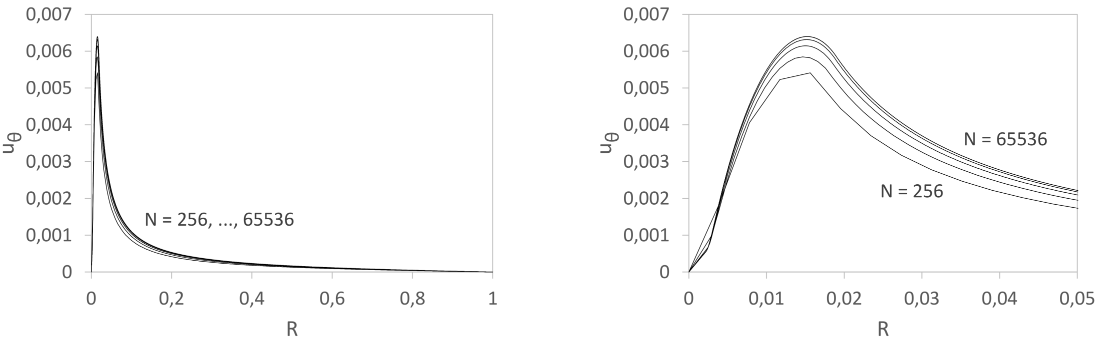


(a) Whole domain (b) Neighborhood of the origin

Figure 2. Tangential displacement $u_\theta$ for the rotationally symmetric solution obtained numerically using $256, 1024, 4096, 16384, 65536$ elements and $\delta = 10^8$.

Fig. 9. In spite of the good qualitative agreement, the maximum value of $u_\theta$ is approximately $0.0065$ in Fig. 2 and $0.0036$ in their Fig. 9. Also, it is not clear from their figure that $u_\theta$ behaves linearly in a vicinity of the center of the disk. In fact, in their figure, $u_\theta$ seems to be negative very close to this center.

In Fig. 3 we show the determinant of the deformation gradient $J \equiv \det(\mathbf{1} + \nabla \mathbf{u})$ calculated from the rotationally symmetric solution obtained with the most refined mesh for a fixed large penalty parameter $\delta$. We also show $J$ calculated from the radially symmetric solution of Fosdick and Royer-Carfagni [2]. Again, Figure 3a refers to the whole domain $(0, R_e)$ and Fig. 3b refers to a vicinity of the origin. We see from Fig. 3a that both curves become indistinguishable as we move away from the origin and from Fig. 3b that, as we approach the center of the disk, $J$ decreases, is equal to $0.1$ in the interval $(0.0022, 0.0190)$, and has very high values for $R < 0.0022$, which indicates that it is singular at $R = 0$. The interval $(0.0022, 0.0190)$ corresponds to the active region $\mathcal{B}_=$ introduced in Eq. (3) and is different from the active region of the radially symmetric solution, given by $(0, 0.0075)$. In addition, $R = 0.0022$ coincides with the radius below which $u_\theta$ is linear in Figure 2.

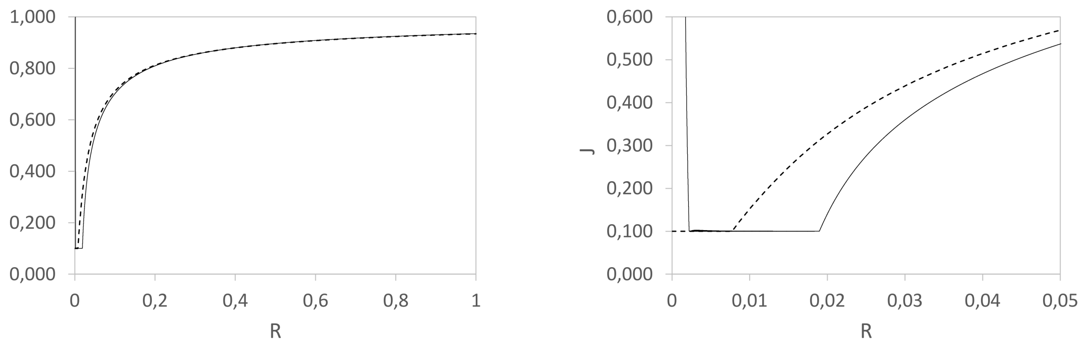


(a) Whole domain (b) Neighborhood of the origin

Rotationally symmetric solution   Radially symmetric solution

Figure 3. Determinant of the deformation gradient, $J$, obtained analytically (dashed line) and numerically (solid line) with 65536 elements and $\delta = 10^8$.

In Fig. 4 we show $\lambda_\delta$, evaluated from Eq. (10), versus $R \in (0, 0.05)$ for a large penalty parameter $\delta$ and different values of $N$. We see that $\lambda_\delta$ takes large, but finite values and it vanishes outside the active region, as expected. The above results are in good qualitative agreement with results shown in Fig. 18 of Fosdick et al. [5]. Quantitatively, both results are of the same order of magnitude, with the maximum value of $\lambda_\delta$ in Fig. 4 being close to 10600 for the most refined mesh and close to 9000 in Fig. 18 of Fosdick et al. [5]. A possible explanation for this difference may be inferred from Fig. 4 itself, where we see that the maximum values of $\lambda_\delta$ vary considerably with $N$.

We have also used the mesh with 65536 elements to calculate the total potential energy functional $\mathcal{E}$, given by Eq. (20), for both the radially symmetric solution and the rotationally symmetric solution, yielding the approximate values of $264.5$ and $256.6$, respectively. Thus, the total potential energy of the rotationally symmetric solution is lower than the corresponding energy of the radially symmetric solution.

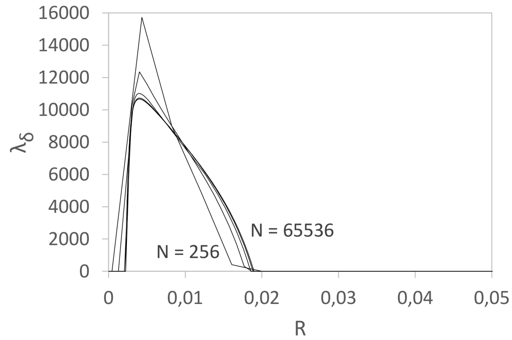


Figure 4. Approximation $\lambda_\delta$ of the Lagrange multiplier for the rotationally symmetric solution using $256, 1024, ..., 65536$ elements and $\delta = 10^8$.

## 5 Conclusions

In this work we have investigated the problem of a cylindrically anisotropic disk in equilibrium with no body force, which is subjected to a prescribed displacement along its external boundary. We have searched for either radially or rotationally symmetric solutions of the associated minimization problem subjected to the injectivity constraint $\det\nabla\mathbf{f} \geq \epsilon > 0$. For this, we have used the penalty formulation proposed by Aguiar [4] together with a finite element procedure defined over a one-dimensional domain, instead of the two-dimensional domain of Fosdick et al. [5]. Our discretization strategy uses linear finite elements and yields a convergent sequence of solutions at a very low computational cost. The sequence converges to a limit function that is close to the radially symmetric solution of the classical linear theory. This result is different from a result reported by Fosdick et al. [5], according to which their numerical solution is close to the radially symmetric solution of the constrained minimization problem. In addition, it is clear from our investigation that a small perturbation must be introduced to obtain the rotationally symmetric solution, for otherwise the solution obtained is radially symmetric. The corresponding total potential energy of the rotationally symmetric solution is lower than that of the radially symmetric solution.

**Acknowledgments**

The first author acknowledges the support of National Council for Scientific and Technological Development (CNPq), grant n$^{\mathrm{o}}$ 420099/2018-2, and the second author wishes to acknowledge the financial support provided by Coordination for the Improvement of Higher Education Personnel (CAPES).

**Authorship statement**

The authors hereby confirm that they are the sole liable persons responsible for the authorship of this work, and that all material that has been herein included as part of the present paper is either the property (and authorship) of the authors, or has the permission of the owners to be included here.

## References

[1] Lekhnitskii, S. G., 1968. *Anisotropic plates*. Gordon & Breach, New York.
[2] Fosdick, R. & Royer-Carfagni, G., 2001. The constraint of local injectivity in linear elasticity theory. *Proceedings of the Royal Society A: Mathematical, Physical and Engineering Sciences*, vol. 457, n. 2013, pp. 2167–2187.
[3] Christensen, R. M., 1994. Properties of carbon fibers. *Journal of the Mechanics and Physics of Solids*, vol. 42, n. 4, pp. 681–695.
[4] Aguiar, A. R., 2006. Local and global injective solution of the rotationally symmetric sphere problem. *Journal of Elasticity*, vol. 84, n. 2, pp. 99–129.
[5] Fosdick, R., Freddi, F., & Royer-Carfagni, G., 2008. Bifurcation instability in linear elasticity with the constraint of local injectivity. *Journal of Elasticity*, vol. 90, n. 1, pp. 99–126.